www.elsevier.com/locate/ijadhadh

Influence of hierarchical micro-micro patterning and chemical modifications on adhesion between aluminum and epoxy

Janne Salstela, Mika Suvanto, Tuula T. Pakkanen

PII: S0143-7496(15)00239-0
DOI: http://dx.doi.org/10.1016/j.ijadhadh.2015.12.036
Reference: JAAD1779

To appear in: *International Journal of Adhesion and Adhesives*

Received date: 24 March 2015
Accepted date: 22 December 2015

Cite this article as: Janne Salstela, Mika Suvanto and Tuula T. Pakkanen Influence of hierarchical micro-micro patterning and chemical modifications o adhesion between aluminum and epoxy, *International Journal of Adhesion an Adhesives,* http://dx.doi.org/10.1016/j.ijadhadh.2015.12.036

Influence of hierarchical micro-micro patterning and chemical modifications on adhesion between aluminum and epoxy.

Janne Salstela[a], Mika Suvanto[a], Tuula T. Pakkanen[a,*]

[a] Department of Chemistry, University of Eastern Finland, P.O. 111, FI-80101, Joensuu, Finland

Abstract

The main target in the study of aluminum-epoxy resin joints was to enhance adhesion by increasing the surface area of aluminum substrates and by chemical functionalizing the aluminum surface to provide coupling points for epoxy resin. The surface area of the aluminum substrates was increased by fabricating microscale structures and hierarchical micro-microstructures by utilizing a micro-mesh printing technique and sandblasting. The effects of silanization with 3-glycidoxypropyltrimethoxysilane (GPTMS) and of oxygen plasma treatment were also investigated. Compared to a smooth surface, the micro-mesh structures improved shear strength by 33% and the hierarchical micro-microstructures by 116%. The utilization of the oxygen plasma treatment and especially the silane modification of the aluminum substrates were found to be effective in promoting adhesion. The specimens modified by combining the chemical or energetic modification method with surface texturing tended to fracture more cohesively than the specimens having a single modification. The hierarchically patterned and plasma and silane modified specimens had so high adhesion that the aluminum substrates started to deflect during the shear strength measurements, thus preventing the evaluation of their maximum strength.

Keywords: Hierarchical surface patterning; Single lap joint; Shear strength; Adhesion; Epoxy; Aluminum; Silane; Plasma

* Corresponding author. Tel +358 504 354 379

Email addresses: tuula.pakkanen@uef.fi (T.T. Pakkanen), janne.salstela@uef.fi (J. Salstela)

1. Introduction

Adhesive joints are widely used in the automotive and aerospace industries instead of conventional welding and mechanical joints . Adhesive joints have many advantages such as flexibility of design, lightness, fast and easy fabrication process, uniform load distribution over the whole bonded area and capability to join dissimilar materials . As with any other method, adhesive jointing methods have their disadvantages which are for example environmental stress caused by the use of chemicals, limited shelf life of the adhesives and, frequently, a requirement for heat curing. Moreover, adhesive joints do not have a high strength towards peeling forces and thus require pretreatment of adherend surfaces to achieve good bonding . When improving adhesion between the adhesive and the substrate, it is important to know the factors having an influence on adhesion. Various adhesion theories have been developed and one of the most commonly referred to are mechanical interlocking, adsorption and chemical bonding theories .

The pretreatment of adherend surfaces can be roughly classified into mechanical, chemical and energetic modifications. Mechanical pretreatments to increase surface area of the metal substrate include for example grit blasting , mechanical abrasion with sandpaper and groove fabrication . Acid etchings , anodizing and the use of coupling agents are the most commonly used methods to functionalize metal substrate surfaces. Especially silanization has been proven to be an effective way to improve adhesion in metal-polymer resin joints. Use of adhesion promoters requires careful selection of the silane. The silane has to have suitable chemical groups to form chemical bonds both to the substrate and the adhesive. For polymer composites, energetic modifications such as plasma and flame treatments have been studied as more environmentally friendly adhesion enhancing methods. The plasma treatment of metal surfaces has been presented as a suitable adhesion promoting technique for metal-polymer resin interfaces . Plasma treatment has also improved the wetting of an aluminum substrate with a silane solution . This suggests that silanes could bind to the aluminum surface more effectively and therefore improve adhesion in aluminum-polymer resin interfaces.

The main target in our study of aluminum-epoxy resin joints was to improve adhesion by increasing the surface area of aluminum substrates and by functionalizing the aluminum surface to provide coupling points

for epoxy resin. In the automotive and aerospace industries, epoxy resins are one of the most commonly used adhesives for aluminum . The epoxy adhesive adsorbs onto the aluminum surface mainly with hydrogen bonds . The functionalization of the aluminum surface by coupling agents could provide an environment where covalent chemical bonding is possible, hence improving adhesion . The use of hierarchical surface structures should also improve the robustness of the adhesive joints because it provides more mechanical interlocking points and larger surface area compared to the corresponding unstructured surface. In nature, hierarchical surface structures have been proven to have good adhesion properties. Probably the most well-known example of nature's hierarchical adhesion promoting structure is the feet of geckos .

In the present paper, new types of microscale and hierarchical micro-microscale surface structures were fabricated on aluminum substrates in order to increase their surface area. The adhesion promoting properties of the surface patternings were investigated with epoxy resin in single lap joints. In addition, the adhesion improvement by using 3-glycidoxypropyltrimethoxysilane and oxygen plasma treatment was studied. The effects of different combinations of the mechanical, chemical and energetic modifications on the adhesion properties of aluminum-epoxy joints were also investigated. The different approaches for improving adhesion between the aluminum substrate and the epoxy adhesive are summarized in Scheme 1.

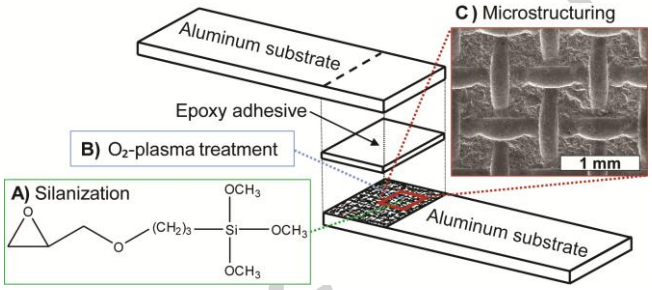

Scheme 1. A) Chemical, B) energetic and C) physical modifications of an aluminum substrate.

2. Materials and methods

2.1. Materials

Commercial EN AW-5754-aluminum was selected as a substrate and Araldite GY 285 Bisphenol F epoxy (Huntsman) resin as an adhesive. Epoxy resin was cured with isophorondiamine (IPDA) curing agent and its relative amount to epoxy was 24.8 w-%. 3-Glycidoxypropyltrimethoxysilane (GPTMS) was used as an adhesion promoter. Curing agent and adhesion promoter were both purchased from Sigma Aldrich and their purities were ≥ 99 % and ≥ 98 %, respectively. Microscale stainless steel metal meshes, used in the microstructuring of substrates, were purchased from Spinea Ltd.

2.2. Specimen preparation, shear strength measurement and fracture investigation

The aluminum substrates (dimensions 3 mm*25 mm*100 mm) were used as received. They were degreased with acetone in an ultrasonic bath for 15 minutes. Mesh printed and sandblasted substrates were degreased after the modification and silanized or plasma treated substrates were degreased before the modification. Epoxy resin was preheated and mixed with a magnetic stirrer at 70 °C and 500 rpm followed by the addition of the diamine curing agent. After the diamine was added, the mixture was further mixed for 3 minutes. Substrates and the diamine/epoxy-mixture were then joined together with a special jig, where adhesive layer thickness, overlap and alignment could be controlled. The adhesive layer thickness was set to 0.2 mm and overlap to 12.5 mm. A schematic representation of the manufactured single lap joint can be seen in Fig. 1. The joined specimens were cured with a curing sequence: 82 °C for 90 minutes and 150 °C for 90 minutes. After curing, the specimens were stabilized overnight in a desiccator followed by shear strength measurement.

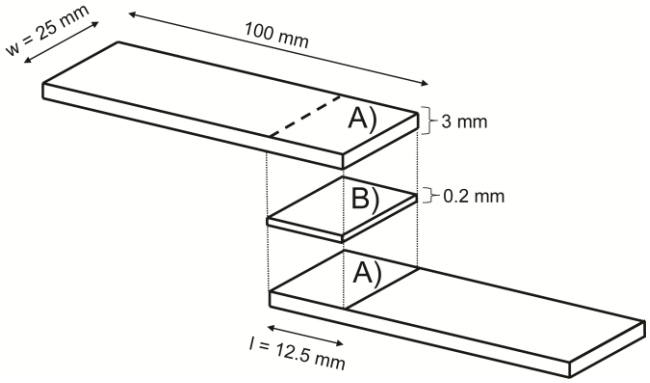

Figure 1. A schematic picture of single lap joint specimen: A) aluminum substrate and B) adhesive layer.

Shear strength measurement using a single lap joint configuration was chosen for the adhesion measurements, because it provided a test system where the effects of different surface structures could be reproducibly measured on a laboratory scale. At least 5 specimens were measured to ensure repeatability. All shear strength measurements were carried out with a Zwick Z010/TH2A material testing machine. The test specimens were fastened by using asymmetrical grips (Zwick/Roell Typ 8306) in order to align the specimens and hence minimize bending and peeling during the test. The crosshead speed was set to 1 mm/s and kept constant. Shear strength P was calculated by using Equation 1.

$$P = \frac{F_{max}}{A} = \frac{F_{max}}{l*w} \quad (1)$$

Where F_{max} is the maximum force applied before total failure, A is the overlap area of the single lap joint specimen, l is the length and w is the width of the overlap area.

The fractured surfaces of single lap joint specimens were examined with an Hitachi S-4800 scanning electron microscope (SEM) and the acceleration voltage was set to 3 kV. All SEM samples were coated with a 4 nm gold layer using a Cressington Sputter Coater 208HR applied with Cressington thickness Controller MTM-20. A visual appearance of the fractured single lap joint specimens was captured with a camera (Sony HDR-SR 11E).

2.3. Physical modification with microstructuring

A mesh-type microstructuring was introduced onto aluminum substrates by a micro-mesh printing technique. The dimensions of the microstructured area were 25 mm*15mm. Mesh sizes of 100 µm, 200 µm and 400 µm

were used in the study. The ratio between the mesh size and the diameter of the mesh wire was approximately the same with all the meshes used in the experiments (See Appendix A, Table A1). Micro-mesh printing was performed with a hydraulic press with a constant pressing time of 1 minute. A supportive stainless steel plate (dimensions 10 mm*40 mm*130 mm) was used in micro-mesh printing to prevent the deformation of specimens. Micro-mesh printing parameters are shown in Table 1 and a schematic picture of the micro-mesh printing set-up is presented in Fig. 2.

Sandblasting was used as a reference technique for microstructuring. The sandblasting pressure was set to 6 bars. The particle size of the quartz sand used in sandblasting was < 1 mm. Sandblasting was performed to a stage where the structured surface of the aluminum substrate had visually lost all its gloss. Hierarchical microstructures were fabricated onto aluminum substrates by using different combinations of micro-mesh printing and sandblasting.

Table 1. Micro-mesh printing parameters.

Mesh size [µm]	Pressing force [kN]	Pressing time [min]
100	35	1
200	33	1
400	30	1

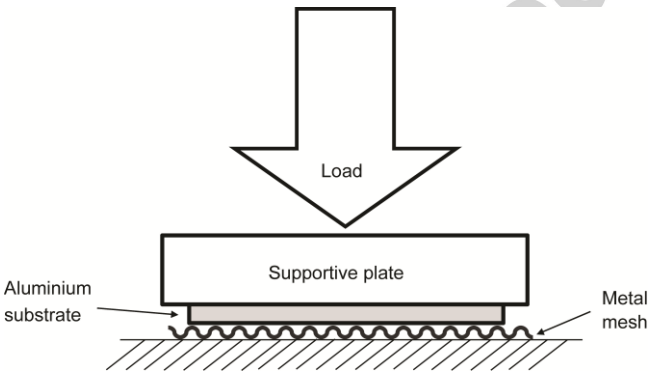

Figure 2. Schematic picture of micro-mesh printing technique.

2.4. Energetic modification with plasma treatment

The degreased aluminum substrates were treated with oxygen-plasma by using an Oxford Instruments Plasmalab80plus-device in RIE-mode. The chamber pressure was set to 100 mTorr, the wafer temperature to

20 °C, the forward power to 30W and the treatment time to 2 minutes. During the plasma treatments, the reflected power was observed to be around 1 W, which means that the adsorbed power was 29 W. An Ar/O_2 gas mixture with different concentrations was introduced into the plasma chamber and controlled by mass flow controllers with oxygen contents of 0%, 10%, 20%, 30%, and 40%. The flow rate of the gas mixture was kept constant and was set to 20 sccm. After the plasma treatment, the aluminum substrates were immediately silanized or fabricated into single lap joint specimens.

2.5. Chemical modification with silanization

Silane was stirred in ethanol solution containing 5 Vol-% of water. The amount of silane in the solution was 0.5-2.5 w-% and the pH of the solution was 7. The silane solution was hydrolyzed for 1 hour while mixing with a magnetic stirrer (500 rpm). After the hydrolysis, the degreased substrates were immersed in the solution for 5 minutes. After the immersion, the silanized substrates were cured at 200 °C for 30 minutes. The silanized substrates were kept in a desiccator overnight before joint fabrication. The hydrolysis and surface reactions of GPTMS are shown in Appendix B Scheme B1.

3. Results and discussion

3.1. Microstructuring

Three different types of micro patterns were fabricated on the aluminum substrates: microstructuring with micro-meshes, hierarchical sandblasting + micro-mesh printing and hierarchical micro-mesh printing + sandblasting. Smooth and sandblasted aluminum substrates were used as references. The microstructuring sequences and the abbreviations of different surface patternings are shown in Table 2.

Table 2. Fabricated microstructures and hierarchical micro-microstructures. Numbers indicate mesh size, e.g. $M^{100}S$ equals to 100 µm mesh printing followed by sandblasting.

Surface	Abbreviation	1. treatment	2. treatment
Smooth	Smooth	-	-
Sandblasted	S	Sandblasting	-
Mesh printed	M^{100} M^{200} M^{400}	Micro-mesh printing	-

Sandblasted + mesh printed	SM^{100} SM^{200} SM^{400}	Sandblasting	Micro-mesh printing
Mesh printed + sandblasted	$M^{100}S$ $M^{200}S$ $M^{400}S$	Micro-mesh printing	Sandblasting

The microstructured aluminum substrates were examined with SEM to evaluate the replication fidelity of the surface patterns. SEM images of the fabricated microstructures are shown in Figs. 3-4.

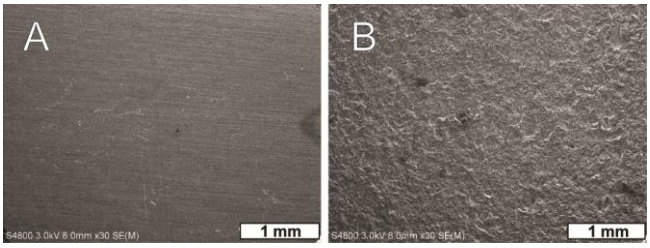

Figure 3. SEM images (magnification of 30x) of A) smooth and B) sandblasted aluminum.

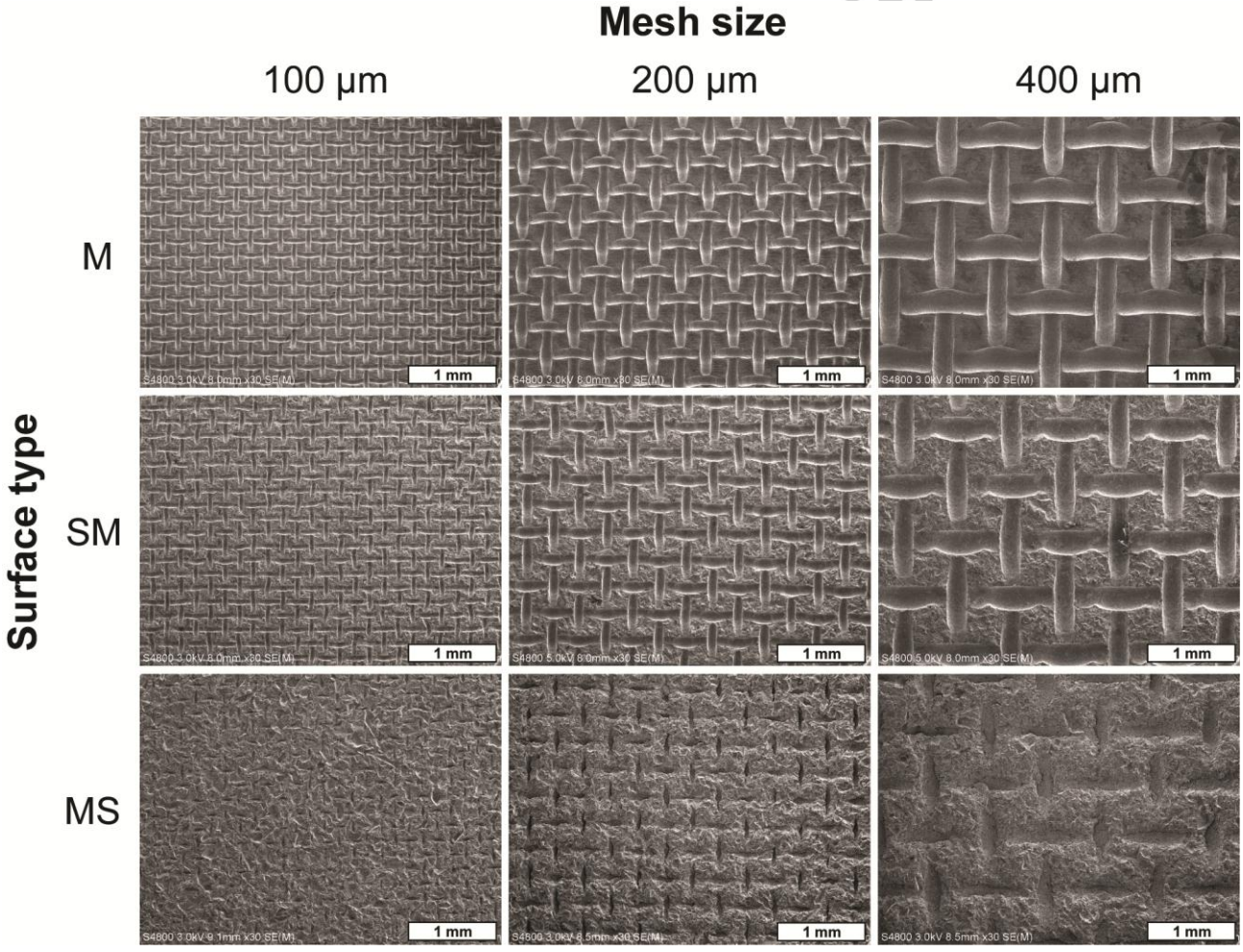

Figure 4. SEM images (magnification of 30x) of M-type, SM-type and MS-type surface structures.

According to Fig. 3, sandblasting of aluminum substrate produces a random microstructure with sharp edges compared to micro-mesh printing (Fig.4), which leads to a very regular pattern with smooth edges. Patterning with micro-meshes (M-type structures) is expected to increase the surface area by 35 % compared to the smooth surface (See appendix A Fig. A1 and Table A1). A major difference between the M-type surfaces was the number of locking points (see appendix A Table A1). The M^{100} surface had the highest number of locking points (38/mm^2) while the M^{400} surface had only a few (2-3/mm^2) (Fig. 4). From the SEM-images of the hierarchical SM structures (Fig. 4), it can be clearly seen how the micro-mesh structure smoothens the random microstructure obtained with sandblasting. However, in the case of the MS structures (Fig. 4), the micro-mesh printed structure almost disappears in the final sandblasting step, especially in the case of the smallest 100 µm mesh sample. On the largest 400 µm mesh pattern, sandblasting only roughens the mesh print throughout the whole printed surface providing a hierarchical structure where larger microstructure (mesh print) is covered with smaller "sub-micro"-structure (sandblasting).

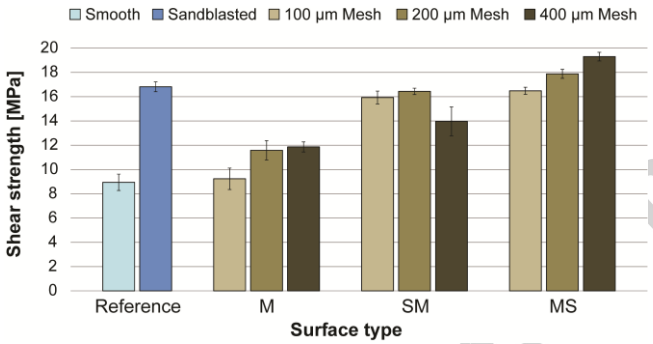

Figure 5. Effect of microstructuring on shear strengths.

The effect of microstructuring on shear strength is shown in Fig. 5. The random sandblast structure gives excellent adhesion properties when compared to the M-type structures. The hierarchical SM-type surfaces had lower adhesion to epoxy than the mere sandblasted surface. This was most probably due to micro-mesh printing which smoothened the structure produced by sandblasting, as seen in Fig. 4. All hierarchical MS-type surfaces had good adhesion properties and moreover, there is a clear correlation between the shear strength and the micro-mesh size. For the $M^{100}S$ and $M^{200}S$ structures, the improvement in adhesion was not high, probably due to the too small micro-mesh structures which epoxy resin cannot wet properly. From the MS-type surfaces, the $M^{400}S$ surface performed the best giving an almost 15% improvement in shear strength

compared to the sandblasted surface. Photographs and SEM images of the fractured single lap joint specimens are shown in Fig. 6.

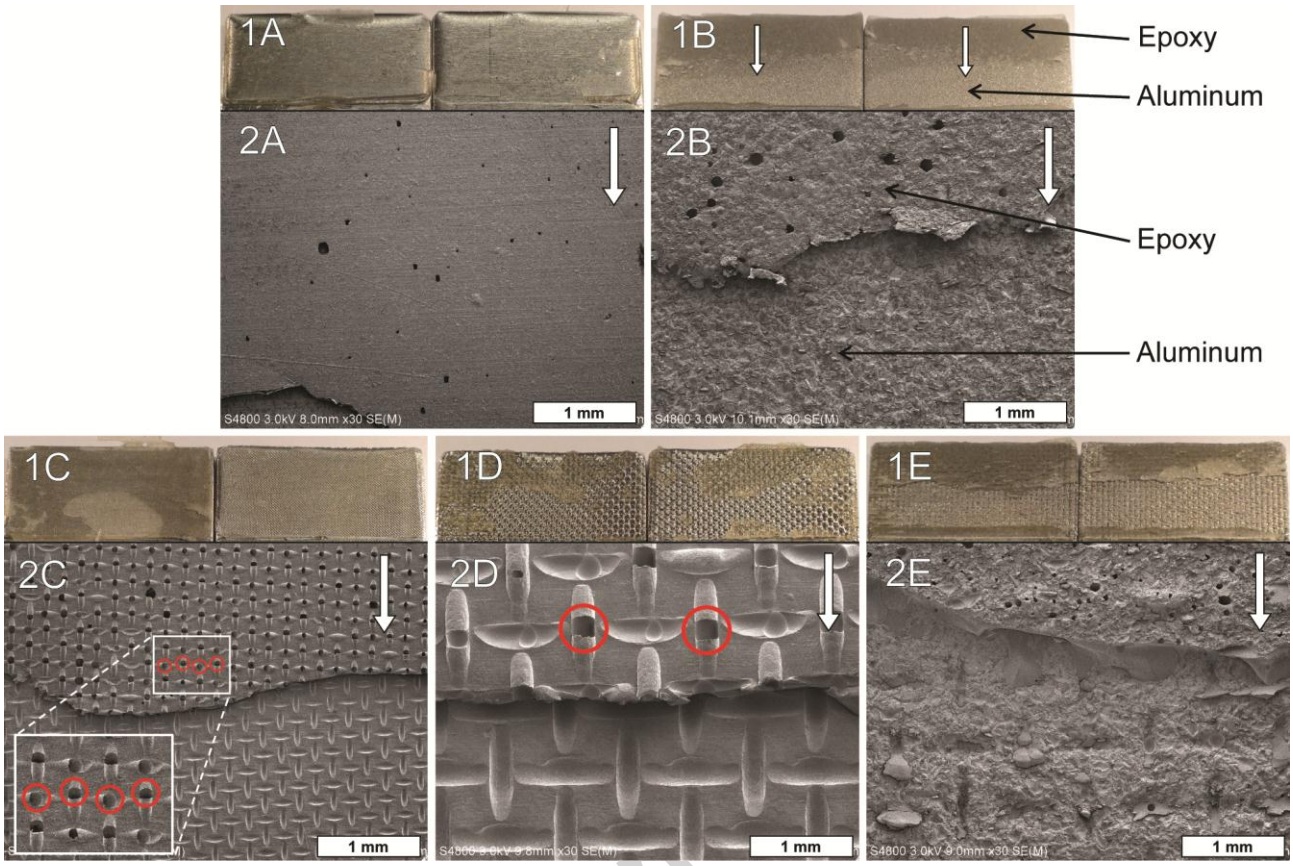

Figure 6. 1) Photographs and 2) SEM-images (magnification of 30x) of fractured A) smooth reference, B) sandblasted reference, C) M^{100}, D) M^{400} and E) hierarchical $M^{400}S$ structured Al/epoxy/Al specimen. White arrows indicate the direction of the stress. The cavities inside the mesh printing is marked with red circles.

On all smooth reference and M-type aluminum surfaces, the cured epoxy tended to fracture adhesively with very clear cut surfaces. In comparison, on the sandblasted and on the hierarchical SM and MS surfaces, the cured epoxy had much rougher shear cuts. When comparing the two M-type surfaces to each other (Fig. 6 C and D), epoxy resin had spread on the M^{400} surface much better than on the M^{100} surface evidenced by a high number of cavities inside cured epoxy of the M^{100} surfaces.

With the M^{400} structured surfaces, cured epoxy fractured cohesively along the mesh wire structure (Fig. 6. 2D), perpendicular to the stress. This effect was not detected on the M^{100} surfaces indicating that the M^{400} structure provided better adhesion to the epoxy layer. All SM-type and $M^{100}S$ surfaces tended to fracture

similarly to the sandblasted surfaces. The failure mode of the $M^{200}S$ and especially the $M^{400}S$ structured specimens was more cohesive. The cohesive fracture can be deduced from the epoxy residues covering the whole aluminum surface (Fig. 6 E). The observed fracture type correlated well with the shear strength data. The best microstructure (M^{400}) and the best hierarchical micro-microstructure ($M^{400}S$) were chosen for further studies.

The shear results of the M-type surface structures correlate well with previous studies of da Silva et al. where they examined the effects of macroscale grooves on the strength of aluminum-epoxy single lap joints. Mere gridlike groove patterns (groove separation 2 mm, groove depth 0.1-0.3 mm) were found to improve adhesion 45% at the best when compared to a smooth surface, while our M^{400} structure improved adhesion by 33%. This suggests that the size of the surface patterns has to be large enough in order for epoxy to penetrate into the micro-pattern.

Sand or grit blasting is known to be an effective way to improve adhesion , , . Grit blasting has been shown to improve the shear strength between aluminum and epoxy adhesive by 50% and 100% , when compared to the corresponding smooth surfaces. These results correlate well with our 100% improvement. Our hierarchical micro-microstructures have not been previously reported in terms of adhesion promoters, but Rider et al. have reported the adhesion promoting effects of hierarchical micro-nano surface structures. When compared to a mere grit blasted surface, the hierarchically micro-nanostructured aluminum-epoxy specimens had up to 100 percent shorter crack lengths in a wedge test. This shows that hierarchical structures have a clear effect on the robustness of adhesively bonded joints.

3.2. Plasma treatment and silanization

For energetic and chemical modifications of aluminum substrate, oxygen plasma treatment and silanization with GPTMS were employed. Plasma treatment parameters were set mild to achieve oxygen deposition on the aluminum surface without etching the surface. Five different O_2 proportions (0-40%) in argon and five different GPTMS contents (0.5-2.5 w-%) in ethanol-water solutions were studied to achieve the optimal modification parameters. Smooth aluminum substrates were used for both studies. The effects of plasma treating and silanization on shear strengths are shown in Figs. 7 and 8.

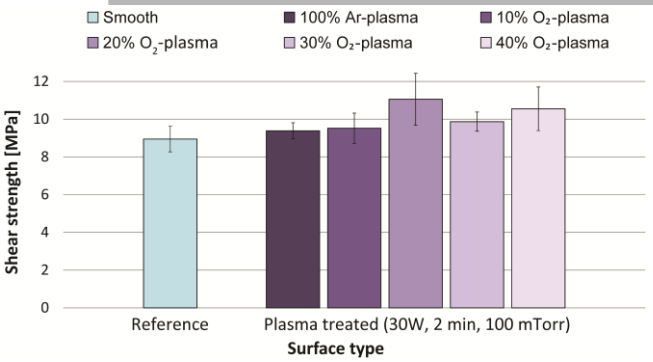

Figure 7. Effect of oxygen content of the plasma gas on shear strengths of smooth Al/epoxy/Al-specimen.

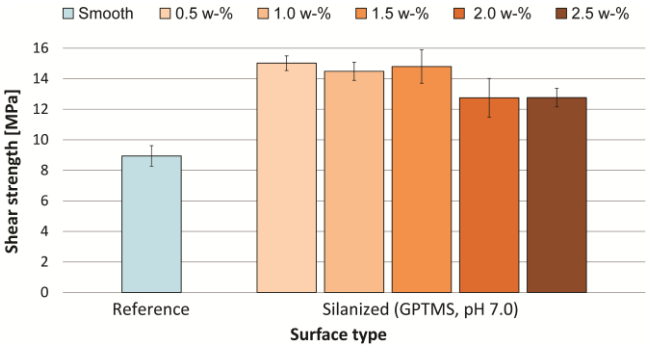

Figure 8. Effect of concentration of alcoholic GPTMS solution on shear strengths of smooth Al/epoxy/Al-specimen.

According to the results shown in Fig. 7, plasma treatment improves adhesion slightly. The effect of different oxygen contents of the plasma on the shear strength was minor. The 20% oxygen content was found to improve adhesion highest, with an almost 24% improvement in shear strength. Silanization with GPTMS improved adhesion up to 68% with very good repeatability. The highest strength was obtained with the low silane content. Qui et al. have reported similar behavior of GPTMS in aluminum-epoxy joints where the lower silane content resulted in the higher shear strength.

Plasma treated and silanized specimens both tended to fracture adhesively in macroscale. On the basis of SEM images of the fractured specimens, the silane treated specimens had microscale shear cuts on the epoxy surfaces (see Fig. 9). The silane treated specimens also had much less cavities inside the cured epoxy indicating better wetting properties of the aluminum surface compared to the untreated (see Fig. 3A) and plasma treated surfaces. For further studies, the 20% oxygen plasma treatment and the silanization with 0.5 w-% GPTMS solution were selected.

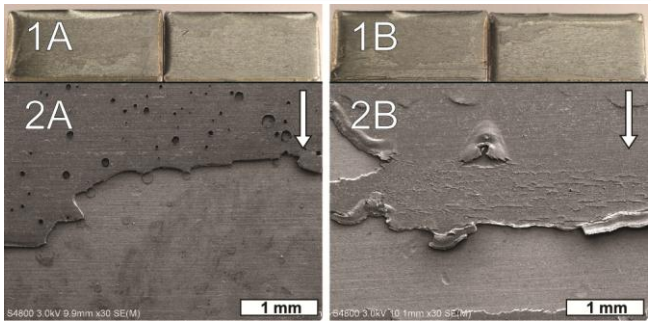

Figure 9. 1) Photographs and 2) SEM-images (magnification of 30x) of fractured A) plasma treated and B) silanized Al/epoxy/Al specimen. White arrows indicate the direction of the stress.

A 24% increase in the shear strength result on the O_2/Ar plasma treatment of aluminum substrate correlates well with the study where the O_2/Ar microwave plasma treatment of steel surfaces increased the tensile strength of steel-epoxy specimens by 20% . Sperandio et al. used air cold plasma with different O_2/N_2 mixtures to enhance the shear strength between aluminum and epoxy. The best shear properties were achieved when aluminum substrates were plasma treated with 20% of O_2.

3.3. Combination of mechanical, energetic and chemical modification

To improve adhesion even further, the mechanical, energetic and chemical modifications used were studied in different combinations. For these hybrid modifications the parameters were chosen on the basis of the present results. Smooth, M^{400}, sandblasted and $M^{400}S$ aluminum surfaces were used with 20% O_2 plasma treatment and silanization with 0.5 w-% GPTMS solution. The effects of hybrid modifications on the shear strength are shown in Fig. 10.

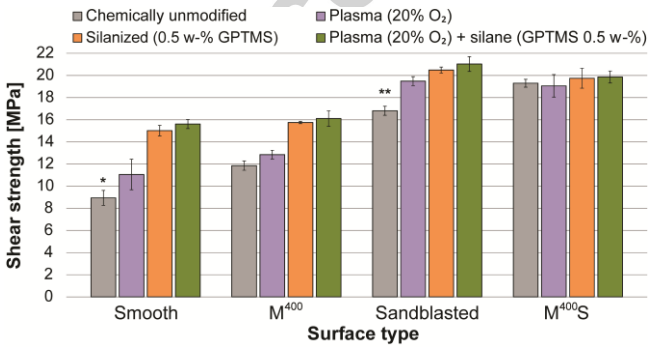

Figure 10. Effect of hybrid modifications on shear strengths in Al/epoxy/Al system. * = smooth reference and ** = sandblasted reference.

The smooth and M^{400} structured hybrid samples having either the silane modification or the combined plasma and silane treatments had effectively the same shear strength values (see Fig. 10). This suggests that silane treatment does not benefit from a regular M^{400} microstructuring. When the functionalization with silane or with the joined plasma + silane treatments are combined with sandblasting, which produces a more random microstructure, adhesion is improved significantly. Unexpectedly, in the case of the hierarchical $M^{400}S$ structures the hybrid modifications did not increase the maximum shear strengths further. All hybrid modified $M^{400}S$ structured specimens had so high adhesion that aluminum substrates started to deflect during the shear strength measurements (see Fig. 11). This prevented the evaluation of the maximum shear strengths of the specimens. During the shear strength measurements, the hybrid modified $M^{400}S$ structured specimens stayed silent till the point of the final fracture. All other specimens produced loud cracking noises throughout the shear strength measurements indicating poor adhesion properties. Macro- and microscale shear phenomena occurred in the fractured joint specimens having the combined plasma and silane modifications as shown in Fig. 12.

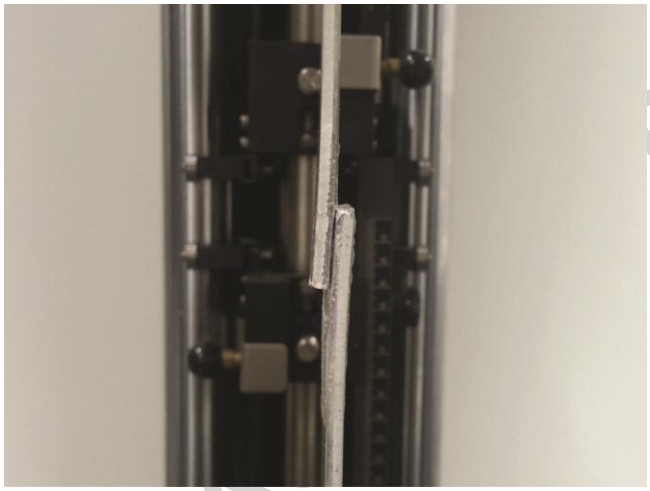

Figure 11. Deflection of the single lap joint specimen (silanized $M^{400}S$ substrates).

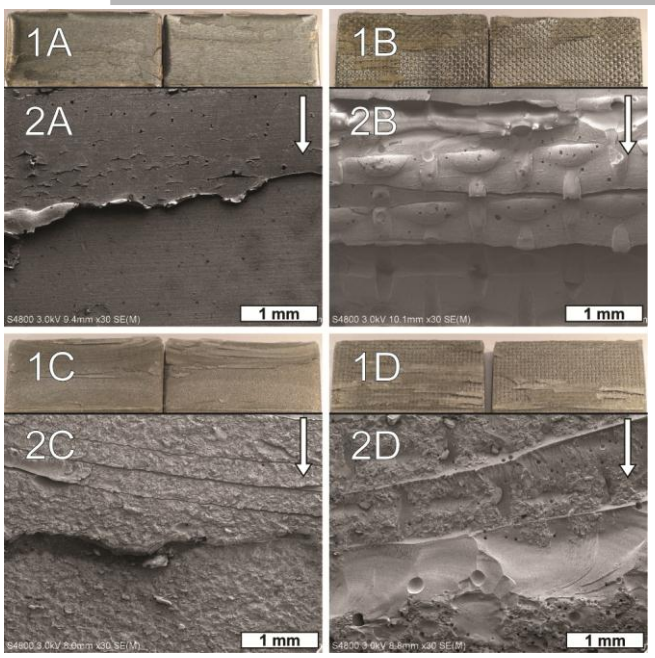

Figure 12. 1) photographs and 2) SEM-images (magnification of 30x) of fractured plasma + silane hybrid modified Al/epoxy/Al specimens on a A) smooth, B) M^{400} structured, C) sandblasted or D) $M^{400}S$ structured aluminum substrate. White arrows indicate the direction of the stress.

Fig. 12 indicates that, the smooth specimen had only microscale shear cuts on the epoxy layer whereas with the M^{400} structured and the sandblasted specimen the shear cuts tended to be in macroscale. This correlated well with the shear strength measurement data. It is also noticeable how the plasma + silane treated specimen had fewer cavities inside the epoxy when compared to the untreated specimen (see Fig. 6), indicating that epoxy resin had wetted the aluminum surface much better. With the $M^{400}S$ structured specimen, the aluminum substrates started to deflect and therefore the epoxy adhesive was experiencing greater peeling forces than shear forces. This could be seen as the epoxy residues were on the opposite end of the contact area when compared to any other fractured single lap joint specimen (see Figs 12 and 13 and Appendix C Fig. C1). It can be assumed that with the hybrid modified $M^{400}S$ structured specimens, the shear strength value should be much higher. Due to the high adhesion and shear properties of the hybrid modified $M^{400}S$ structured specimen, the test system started to fail. The deflection of the single lap joint shear specimens under high loads is a reported phenomenon , , , , and is known to have an effect on the shear strength measurements.

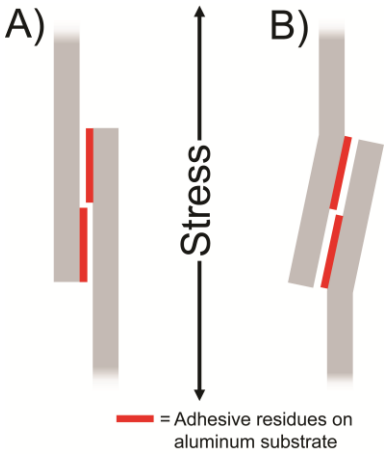

Figure 13. Schematic illustration of the fractured A) typical hybrid modified specimen and B) hybrid modified $M^{400}S$ structured single lap joint specimen.

4. Conclusions

The target of this study was to improve adhesion between aluminum substrate and epoxy adhesive by increasing the surface area and number of locking points of the aluminum substrates with microscale mesh structuring and hierarchical micro-micro surface patterns. The aluminum substrate surfaces were also chemically modified with plasma treatment and silanization in order to functionalize the aluminum surface. The objective was achieved: microscale mesh structuring and especially hierarchical micro-microstructuring were found to be effective tools to improve the adhesion properties of the studied system. Microstructuring, though, had its limitations: the mesh size (and mesh wire diameter) had to be large enough so that the epoxy adhesive could fill in the fabricated microstructure. Silanization with GPTMS was found to be an excellent adhesion promoting method for all studied surface structures whereas plasma treatment had only a minor effect. On combining the hierarchical $M^{400}S$ pattern with the plasma and/or silane hybrid modifications, adhesion was found to be so high that the aluminum substrates started to deflect during the shear strength measurements, thus preventing the evaluation of the maximum shear strength values. It can be concluded that hierarchical micro-microstructuring provides a proper platform for adhesive to produce strong and robust joints between metal parts.

Acknowledgements

Financial support from the Finnish Funding Agency for Technology and Innovation (Tekes), Inorganic Materials Chemistry Graduate Program (EMTKO) and the European Union/European Regional Development Fund within its SAM project are gratefully acknowledged.

References

[1] S. Y. Park, W. J. Choi, H. S. Choi, H. Kwon and S. H. Kim, "Recent Trends in Surface Treatment Technologies for Airframe Adhesive Bonding Processing: A Review (1995-2008)," The Journal of Adhesion, vol. 86, no. 2, pp. 192-221, 2010.

[2] F. Awaja, M. Gilbert, G. Kelly, B. Fox and P. j. Pigram, "Adhesion of polymers," Progress in Polymer Science, vol. 34, no. 9, pp. 948-968, 2009.

[3] A. Baldan, "Review Adhesively-bonded joints and repairs in metallic alloys, polymers and composite materials: Adhesives, adhesion theories and surface pretreatment," Journal of Materials Science, vol. 39, pp. 1-49, 2004.

[4] A. M. Pereira, J. M. Ferreira, F. V. Antunes and P. J. Bártolo, "Analysis of manufacturing parameters on the shear strength of aluminium adhesive single-lap joints," Journal of Materials Processing Technology, vol. 210, no. 4, pp. 610-617, 2010.

[5] M. W. Rushfort, P. Bowen, E. McAlpine, X. Zhou and G. E. Thompson, "The effect of surface pre treatment and moisture on the fatigue performance of adhesively-bonded aluminum," Journal of Materials Process and Technology, Vols. 153-154, pp. 359-365, 2004.

[6] T. A. Barnes and I. R. Pashby, "Joining techniques for aluminium spaceframes used in automobiles: Part II — adhesive bonding and mechanical fasteners," Journal of Materials Processing Technology, vol. 99, no. 1-3, pp. 72-79, 2000.

[7] S. G. Prolongo and A. Ureña, "Effect of surface pre-treatment on the adhesive strength of epoxy–aluminium joints," International Journal of Adhesion & Adhesives, vol. 29, no. 1, pp. 23-31, 2009.

[8] A. Baldan, "Adhesion Phenomena in Bonded Joints," International Journal of Adhesion and Adhesives, vol. 38, pp. 95-116, 2012.

[9] A. F. Harris and A. Beevers, "The effects of grit-blasting on surface properties for adhesion," International Journal of Adhesion and Adhesives, vol. 19, no. 6, pp. 445-452, 1999.

[10] M. Shahid and S. A. Hashim, "Effect of surface roughness on the strength of cleavage joints," International Journal of Adhesion and Adhesives, vol. 22, no. 3, pp. 235-244, 2002.

[11] J. G. Kim, I. Choi and D. G. Lee, "Contact angle and wettability of hybrid surface treated metal adherends," Journal of Adhesion Science and Technology, vol. 27, no. 7, pp. 794-810, 2013.

[12] L. F. da Silva, N. Ferreira, V. Richter-Trummer and E. Marques, "Effect of grooves on the strength of adhesively bonded joints," International Journal of Adhesion & Adhesives, vol. 30, no. 8, pp. 735-743, 2010.

[13] D. G. Lee, J. W. Kwon and D. H. Cho, "Hygrothermal effects on the strength of adhesively bonded joints," Journal of Adhesion Science and Technology, vol. 12, no. 11, pp. 1253-1275, 1998.

[14] J. S. Zhang, X. H. Zhao, Y. Zuo and J. P. Xiong, "The bonding strength and corrosion resistance of aluminium alloy by anodizing treatment in a phosphoric acid modified boric acid/sulfuric acid bath," Surface & Coatings Technology, vol. 202, no. 14, pp. 3149-3156, 2008.

[15] G. W. Clitchlow, K. A. Yendall, D. Bahrani, A. Quinn and F. Andrews, "Strategies for the replacement of chromic acid anodising for the structural bonding of aluminium alloys," International Journal of Adhesion and Adhesives, vol. 26, no. 6, pp. 419-453, 2006.

[16] M. Esfandeh, S. M. Mirabedini and M. T. Pazokifard, "Study of silicone coating adhesion to an epoxy undercoat using silane compounds: Effect of silane type and application method," Colloids and Surfaces A: Physicochemical and Engineering Aspects, vol. 302, no. 1-3, pp. 11-16, 2007.

[17] M. Mohseni, M. Mirabedini, M. Hashemi and G. E. Thompson, "Adhesion performance of an epoxy clear coat on aluminum alloy in the presence of vinyl and amino-silane primers," Progress in Organic Coatings, vol. 57, no. 4, pp. 307-313, 2006.

[18] F. Deflorian, S. Rossi and L. Fedrizzi, "Silane pre-treatments on copper and aluminium," Electrochimica Acta, vol. 51, no. 27, pp. 6097-6103, 2006.

[19] R. Wolf and A. C. Sparavigna, "Role of Plasma Surface Treatments on Wetting and Adhesion," Engineering, no. 2, pp. 397-402, 2010.

[20] J. H. Ku, I. H. Jung, K. Y. Rhee and S. J. Park, "Atmospheric pressure plasma treatment of polypropylene to improve the bonding strength of polypropylene/aluminum composites," Composites Part B: Engineering, vol. 45, no. 1, pp. 1282-1287, 2013.

[21] B. Lapèíková, L. Lapèík Jr., P. Smolka, R. Dlabaja and D. Hui, "Application of radio frequency glow discharge plasma for enhancing adhesion bonds in polymer/polymer joints," Journal of Applied Polymer Science, vol. 102, no. 2, pp. 1827-1833, 2006.

[22] A. P. Pijpers and R. J. Meier, "Adhesion behaviour of polypropylenes after flame treatment determined by XPS (ESCA) spectral analysis," Journal of Electron Spectroscopy and Related Phenomena, vol. 121, no. 1-3, pp. 299-313, 2001.

[23] J. G. Kim, I. Choi, D. G. Lee and I. S. Seo, "Flame and silane treatments for improving the adhesive bonding characteristics of aramid/epoxy composites," Composite Structures, vol. 93, no. 11, pp. 2696-2705, 2011.

[24] N. Saleema and D. Gallant, "Atmospheric pressure plasma oxidation of AA6061-T6 aluminum alloy surface for strong and durable adhesive bonding applications," Applied Surface Science, vol. 282, pp. 98-104, 2013.

[25] J. A. Ting, L. M. Rosario, M. C. Lacdan, H. V. Lee, J. C. De Vero, H. J. Ramos and R. B. Tumlos, "Enhanced adhesion of epoxy-bonded steel surfaces using O2/Ar microwave plasma treatment," International Journal of Adhesion and Adhesives, vol. 40, pp. 64-69, 2013.

[26] C. Sperandio, J. Bardon, A. Laachachi, H. Aubriet and D. Ruch, "Influence of plasma surface treatment on bond strength behaviour of an adhesively bonded aluminium-epoxy system," International Journal of Adhesion and Adhesives, vol. 30, no. 8, pp. 720-728, 2010.

[27] H. J. Chung, K. Y. Rhee, B. S. Han and Y. M. Ryu, "Plasma treatment using nitrogen gas to improve bonding strength of adhesively bonded aluminum foam/aluminum composite," Journal of Alloys and Compounds, vol. 459, no. 1-2, pp. 196-202, 2008.

[28] W. Polini and L. Sorrentino, "Adhesion of a protective coating on a surface of aluminium alloy treated by air cold plasma," International Journal of Adhesion and Adhesives, vol. 27, no. 1, pp. 1-8, 2007.

[29] B. Díaz-Benito and F. Velasco, "Atmospheric plasma torch treatment of aluminium: Improving wettability with silanes," Applied Surface Science, vol. 287, pp. 263-269, 2013.

[30] T. Semoto, Y. Tsuji and K. Yoshizawa, "Molecular Understanding of the Adhesive Force between a Metal Oxide Surface and an Epoxy Resin," The Journal of Physical Chemistry, vol. 115, no. 23, pp. 11701-11708, 2011.

[31] J. Qui, E. Sakai, L. Lei, Y. Takarada and S. Murakami, "Improving the shear strength by silane treatments of aluminum for direct joining of phenolic resin," Journal of Materials Processing Technology, vol. 212, no. 11, pp. 2406-2412, 2012.

[32] K. Liu and L. Jiang, "Bio-inspired design of multiscale structures for function integration," Nano Today, vol. 6, no. 2, pp. 155-175, 2011.

[33] K. K. B. Hon, L. Li and I. M. Hutchings, " Direct writing technology—Advances and developments," CIRP Annals - Manufacturing Technology, vol. 57, no. 2, pp. 601-620, 2008.

[34] H. Gao, X. Wang, H. Yao, S. Gorb and E. Artz, " Mechanics of hierarchical adhesion structures of geckos," Mechanics of Materials, vol. 37, no. 2-3, pp. 275-285, 2005.

[35] G. W. Critchlow and D. M. Brewis, "Review of surface pretreatments for aluminium alloys," International Journal of Adhesion and Adhesives, vol. 16, no. 4, pp. 255-275, 1996.

[36] A. Hafeti, S. Mohagheghi and A. Kianvash, "The effect of silane layer drying temperature on epoxy coating adhesion on silane-pretreated aluminum substrate," Journal of Coatings Technology and Research, vol. 10, no. 5, pp. 743-747, 2013.

[37] A. N. Rider and D. R. Arnott, "Boiling water and silane pre-treatment of aluminium alloys for durable adhesive bonding," International Journal of Adhesion and Adhesives, vol. 20, no. 3, pp. 209-220, 2000.

[38] L. F. M. da Silva and A. Öchsner, Modelling of adhesively bonded joints, Berlin Heidelberg: Springer-Verlag, 2008.

[39] F. M. da Silva, P. J. C. Neves, R. D. Adams and J. K. Spelt, "Analytical models of adhesively bonded joints—Part I: Literature survey," International Journal of Adhesion and Adhesives, vol. 29, no. 3, pp. 319-330, 2009.

[40] G. Belingardi, L. Goglio and A. Tarditi, "Investigating the effect of spew and chamfer size on the stresses in metal/plastics adhesive joints," International Journal of Adhesion and Adhesives, vol. 22, no. 4, pp. 273-282, 2002.

[41] X. Zhao, R. Adams and L. da Silva, "A new method for the determination of bending moments in single lap joints," International Journal of Adhesion and Adhesives, vol. 30, no. 2, pp. 63-71, 2010.

[42] T. Silva and L. Nunes, "A new experimental approach for the estimation of bending moments in adhesively bonded single lap joints," International Journal of Adhesion and Adhesives, vol. 54, no. 10, pp. 13-20, 2014.

Figure captions

Scheme 1. A) Chemical, B) energetic and C) physical modifications of an aluminum substrate.

Figure 1. A schematic picture of single lap joint specimen: A) aluminum substrate and B) adhesive layer.

Figure 2. Schematic picture of micro-mesh printing technique.

Figure 3. SEM images (magnification of 30x) of A) smooth and B) sandblasted aluminum.

Figure 4. SEM images (magnification of 30x) of M-type, SM-type and MS-type surface structures.

Figure 5. Effect of microstructuring on shear strengths.

Figure 6. 1) Photographs and 2) SEM-images (magnification of 30x) of fractured A) smooth reference, B) sandblasted reference, C) M^{100}, D) M^{400} and E) hierarchical $M^{400}S$ structured Al/epoxy/Al specimen. White arrows indicate the direction of the stress. The cavities inside the mesh printing is marked with red circles.

Figure 7. Effect of oxygen content of the plasma gas on shear strengths of smooth Al/epoxy/Al-specimen.

Figure 8. Effect of concentration of alcoholic GPTMS solution on shear strengths of smooth Al/epoxy/Al-specimen.

Figure 9. 1) Photographs and 2) SEM-images (magnification of 30x) of fractured A) plasma treated and B) silanized Al/epoxy/Al specimen. White arrows indicate the direction of the stress.

Figure 10. Effect of hybrid modifications on shear strengths in Al/epoxy/Al system. * = smooth reference and ** = sandblasted reference.

Figure 11. Deflection of the single lap joint specimen (silanized $M^{400}S$ substrates).

Figure 12. 1) photographs and 2) SEM-images (magnification of 30x) of fractured plasma + silane hybrid modified Al/epoxy/Al specimens on a A) smooth, B) M^{400} structured, C) sandblasted or D) $M^{400}S$ structured aluminum substrate. White arrows indicate the direction of the stress.

Figure 13. Schematic illustration of the fractured A) typical hybrid modified specimen and B) hybrid modified $M^{400}S$ structured single lap joint specimen.

Appendix A: Approximation of the relative increase of surface area of the M-type surfaces.

The relative increase of surface area of the M-type surfaces was approximated by comparing surface areas of the micro-mesh printed and reference surfaces (Fig. A1). The ratio R between the micro-mesh structured and reference surface areas are shown in Table A1.

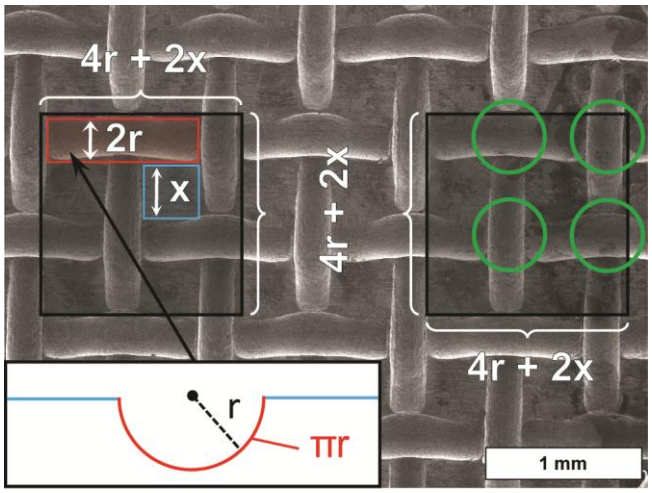

$$R = \frac{A_{micro}}{A_{ref.}} = \frac{4x^2 + 4(2x+2r)\pi r}{(4r+2x)^2}$$

$$N = \frac{\text{No. of lock. points}}{A_{ref.}} = \frac{4}{(4r+2x)^2}$$

Figure A1. Determination of the surface areas for M^{400} surface. Locking points are marked with green circles.

Table A1. Determination of the relative increase of surface area of the M-type surfaces, where x is mesh size, r is radius of mesh wire, β is the ratio between mesh size and mesh wire diameter, R is the ratio between the micro-mesh structured area and the corresponding smooth area and N is the number of locking points in area of 1 mm^2.

Surface	x [µm]	r [µm]	β = x/2r	R	N [1/mm^2]
M^{100}	100	31.3	1.60	1.35	38
M^{200}	200	56.3	1.77	1.34	10
M^{400}	400	118.8	1.68	1.35	2-3

Appendix B: The hydrolysis of GPTMS and its reactions on the surface of aluminum substrate

3-Glycidoxypropyltrimethoxysilane is hydrolyzed in an aqueous solution to form silanols which are then introduced on the aluminum surface where they form covalent bonds to the surface. Then the curing process results in formation of siloxane bridges (See Scheme B1).

1) The hydrolysis of the alkoxygroups to form silanols

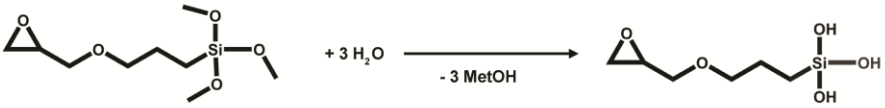

2) Reactions of the silanols with the hydroxyl groups of the surface of aluminum substrate and formation of siloxane brigdes

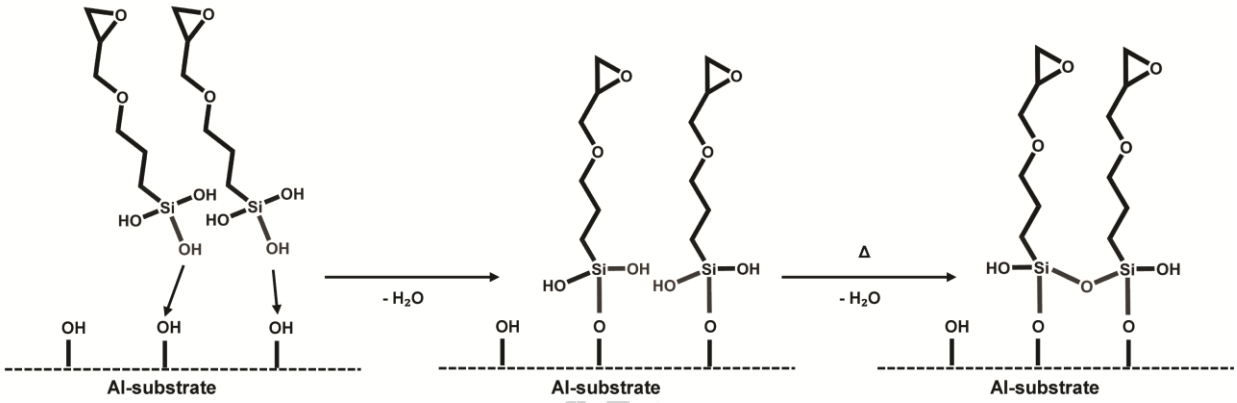

Scheme B1. The hydrolysis of GPTMS and the reactions of hydrolyzed GPTMS on the surface of aluminum substrate [1], [2], [3].

References

[1] P. Walker, "Silane and Other Adhesion Promoters in Adhesive Technology" In: A. Pizzi, K. Mittal (Eds.), Handbook of Adhesive Technology, 2nd ed., Marcel Dekker, USA, 2003, pp. 17

[2] K. Weissenbach, H. Mack, "Silane Coupling Agents" In: M. Xanthos (Ed.), Functional Fillers for Plastincs, Wiley VCH Verlag, Germany, 2005, pp. 59-84.

[3] Y. Xie, C.A.S. Hill, Z. Xiao, H. Militz, C. Mai, "Silane coupling agents used for natural fiber/polymer composites: A review", Composites Part A: Applied Science and Manufacturing, vol. 41, no. 7, pp. 806-819, 2010

Appendix C: Fracture analysis of hierarchically $M^{400}S$ patterned Al/epoxy/Al specimens

With the $M^{400}S$ patterned Al/epoxy/Al specimens, the plasma and/or silane treated aluminum substrates started to deflect in the shear strength measurements. This caused peeling forces to the epoxy adhesive and therefore the epoxy residues were in the opposite end of the contact area when compared to the unmodified $M^{400}S$ patterned Al/epoxy/Al specimens (Fig. C1).

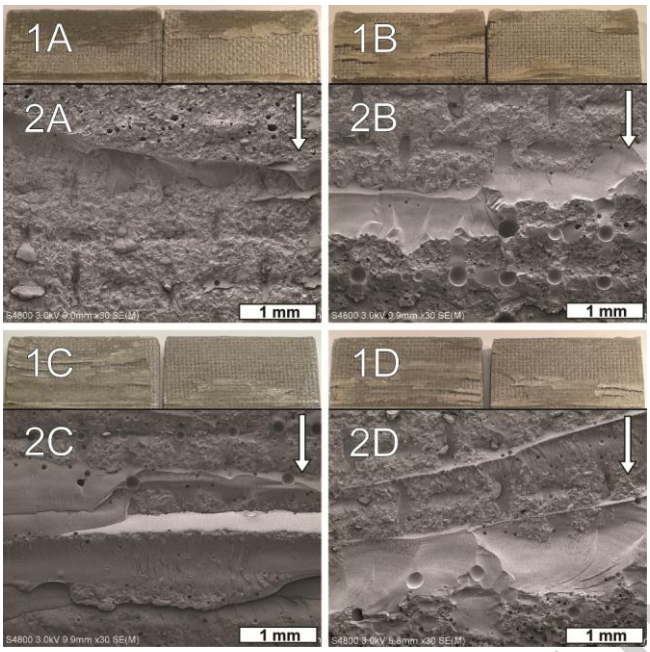

Figure C1. 1) Photographs and 2) SEM-images (magnification 30x) of fractured hierarchically $M^{400}S$ patterned A) unmodified, B) plasma treated, C) silane treated or D) combined plasma + silane treated Al/epoxy/Al specimen. White arrows indicate the direction of the stress.